ISSN 0005–1144
ATKAAF 44(3–4), 147–153 (2003)

Zoran Blažević, Igor Zanchi, Ivan Marinović

Satellite Propagation Channel Analysis via Ray-Tracing Simulation

UDK 621.391.8:629.783
IFAC IA 5.8.3

Preliminary communication

The paper deals with a satellite propagation channel analysis via powerful methods such as ray-tracing, uniform geometrical theory of diffraction and Fourier Transform, already confirmed in various scientific literature. These procedures are easily programmable, and thus can be used as basis for analysing software of various radio channels. In order to present theirs suitability, an example of radio channel of Low-Earth Orbit satellite that emits at central frequency 1625 MHz at various elevation angles (illuminated and shadow zone) is exploited. Accordingly, the diagrams of impulse response and Doppler power spectra are shown and commented. It can be concluded that presented simulation can be successfully applied for multipath radio channel analysis, especially when fundamental channel parameters such as coherence bandwidth or coherence time are to be determined.

Key words: satellite propagation channel, ray-tracing, uniform geometrical theory of diffraction, impulse response, Doppler spectrum

1 INTRODUCTION

Satellite radio systems of today serve in a wide spectrum of human activities like communication, positioning, telemetry, meteorology, etc. However, in real radio environments, regardless of the particular application, various propagation effects strongly influencing the received signal pattern represent limitation in the quality of service (QoS). Thus, in order to determine the best methods for combat against those effects, first the propagation channel parameters as path losses, attenuation rate [1], then mean delay, delay spread, delay interval, delay window [4, 5, 11, 12], or coherence bandwidth and coherence time [4–7, 11] and so forth needs to be known. Since they are easily derived from the radio channel impulse response and Doppler power spectrum statistics [11], the only issue that must be solved is how to obtain the most accurate channel transfer function's data. Those data could be gathered by measurements or by theoretical calculation assuming that enough sufficiently accurate geometrical and electrical parameters of radio environment are provided.

The purpose of the following text is thus to determine a possibility for realistic simulation of satellite radio channels concerning a special case of receivers in built-up areas. The results of such an analysis may serve as foundation for creating efficient satellite mobile radio systems. Accordingly, in chapter 2, the Low-Earth Orbit (LEO) satellite radio channel [1] is modelled in wide-band according to »ray-tracing« and the Uniform Geometrical Theory of Diffraction (UGTD) [9]. Simulation via Wide-Band Propagation Measurement System (WPMS) procedure [2, 3] and Fourier Transform (FT) [8] and analysis of gained results follows in chapter 3.

2 SATELLITE PROPAGATION CHANNEL MODELLING

The geometry of satellite channel model is taken over from [1], where the case of LEO satellite emitting at frequency 1625 MHz from its orbit 720 km above Earth with orbital period of 110 min had been analysed. As channel model is well described in [1], for purpose of this analysis the model is only briefly explained in following text.

In order to compensate the influence of troposphere refraction, an equivalent Earth model for standard atmosphere is used. Such model for a fixed satellite elevation angle $\alpha < 90$ with zoomed receiver (Rx) environment is presented on Figure 1. Due to more precise simulation, instead of the constant effective Earth radius of 4/3 r_Z used in [1], one presented here is corrected with satellite elevation angle α as (see App. A):

$$r_{Zef} = \frac{4}{4 - |\cos\alpha|} r_Z . \tag{1}$$

(Absolute value of the cosine is taken due to fact that the domain of angle α is extended from range $[0, \pi/2]$ to $[0, \pi]$ for simulation purposes.) Note that the influence of the ionosphere may be neglected due to high central frequency [10].

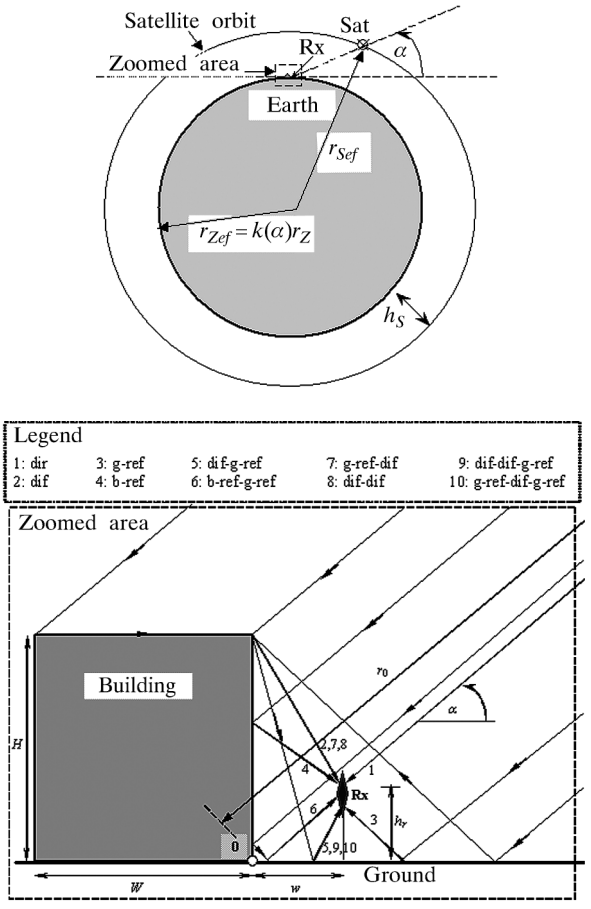

Fig. 1 Radio environment geometry relative to the receiver radio environment and the equivalent Earth model for a satellite elevation angle α

The rays single and multiple diffracted (diff) from the building (b) and/or reflected (ref) from the building (b) and/or ground (g) up to third order are included in the multipath model where plane wave incident to a perfectly conducting building and receiver is assumed [1]. Also, rays that contribute to overall power in receiving point Rx for particular situation described by the figure are emphasized. All in all, there are twelve multipath wave rays possible in various combinations while satellite crosses its way from rise until set relative to fixed receiver on Earth surface. The radio channel analysis that follows is only briefly explained in App. B, as more detailed theory may be found in [1, 7, 10, 11] and other stated references.

3 A CHANNEL SIMULATION AND ANALYSIS

The example of LEO satellite channel at central frequency $f_0 = 1\,625$ MHz for a vertically polarized transmission, for dimensions of building geometry $W \times H = (20 \times 30)$ m^2, the receiver-to-building distance $w = 8$ m and receiver height $h_r = 3$ m was simulated. The satellite emits from orbit $h_S = 720$ km above Earth. The orbital period of the satellite is 110 min, the same as in [1]. The earth radius value applied in this example is $r_Z = 6366$ km. The building and ground permittivity is selected to be 10 and $15 + j \cdot 90/f$ [1], respectively (f is frequency in megahertz). A channel analysis for the satellite elevation angles $\alpha = 45$ (illuminated zone) and $\alpha = 135$ (shadow zone) relative to the receiver is represented here by its frequency pattern in 500 MHz band, impulse response, i.e. time domain path loss, Doppler spectrum and relative power in frequency domain (see App. B).

From frequency patterns on Figure 2 one cannot clearly distinguish the channel characteristics. It is however very clear that the receiver electronics in both cases is more or less confronted against serious frequency selective fading.

On the contrary, a much more vivid view is presented by the channel impulse response on Figure 3, obtained by 4096-point inverse FT with system resolution 4 ns (1,2 m). The reference delay is determined by an arbitrary choice of distance r_0 away from the point »O« marked by the small circle on Figure 1 in a direction toward satellite, which is se-

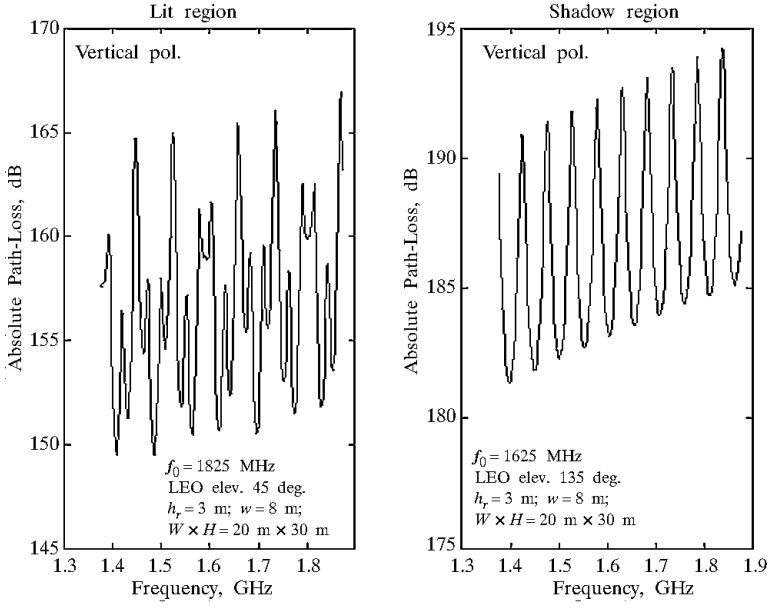

Fig. 2 Frequency pattern of LEO satellite channel in a 500 MHz range around the central frequency 1 625 MHz for a vertically polarized transmission in the illuminated and the shadow area, $(W \times H) = (20 \times 30)$ m^2, $h_r = 3$ m, $w = 8$ m

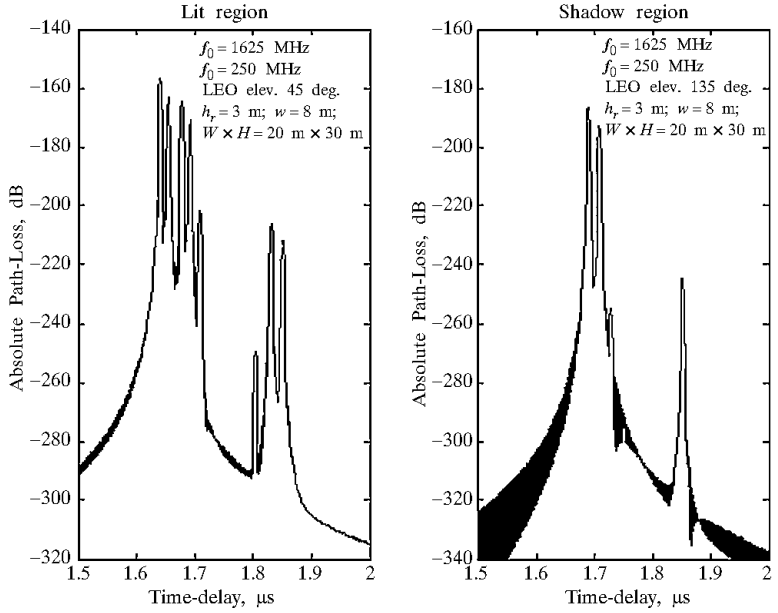

Fig. 3 Time domain path loss for situations according to Figure 2, referent phase 500 m from point »O« in a direction to the satellite, $h_r = 3$ m, $w = 8$ m, clock frequency $f_C = 250$ MHz

lected to be 500 m in our case. The power and time-of-arrival (TOA) of particular wave ray are now easily extracted, since each one is pointed out as a distinct peak in the time domain characteristic. Thus, corresponding rays marked on Figure 2 are immediately recognized but, nevertheless, with finite resolution. The relative power in frequency domain is obtained via FT of the impulse response envelope and presented on Figure 4.

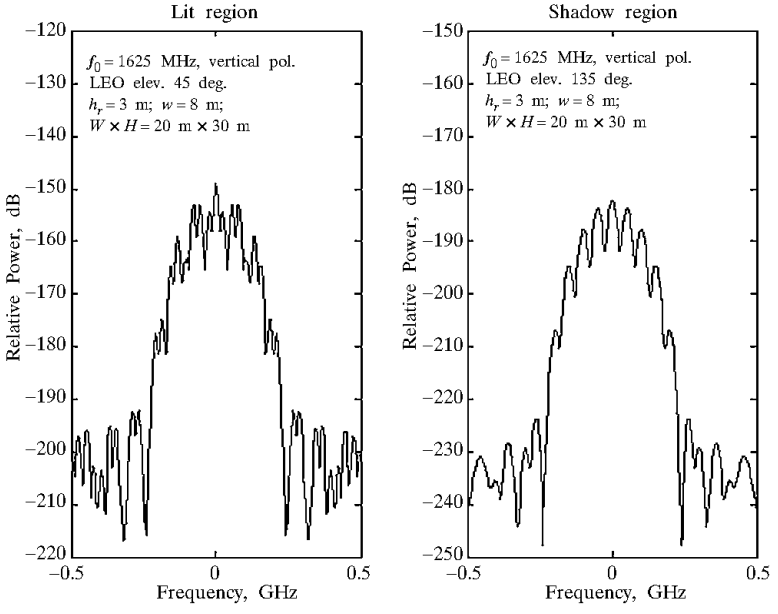

Fig. 4 Relative power in frequency domain of the LEO satellite channel for vertical polarization in illuminated and shadow area, $h_r = 3$ m, $w = 8$ m

Observing Doppler power spectra presented on Figure 5 provides a view from different angle. From displayed Doppler spectra one may immediately conclude about the arrival angles of incoming rays. Those curves are obtained using the 2048-point time domain FT in narrow-band and 1024-point frequency domain inverse FT and then the time domain 512-point FT in wide--band, under an assumption that the receiver Rx departures from the building with speed 90 km/h (25 m/s). For the sake of simplicity, the satellite is assumed fixed. The step used for FT both times equals to a half of the transmitted signal wavelength in order to cover whole possible Doppler frequency shift range. While the satellite is in illuminated region, it is clear that there is one group of rays arriving in front of the receiver with positive Doppler frequency shift and one group of rays coming from its rear with negative Doppler shift. On the contrary, for satellite in shadow region there is only one group of rays arriving to the receiver from the back, which exists mainly as consequence of scattering from the building. As we can see, from obtained spectral curves presented on Figure 5 one may readily conclude about incident angles of rays or group of rays relative to the receiver's direction.

It can be noted that the resolution limit introduced by the WPMS due to the fact that some rays in the impulse response possess practically same delay, may be overcome by measuring the Doppler spectrum at a constant receiver speed for given satellite elevation. Obviously, by combining conclusions derived from the impulse response and Doppler spectrum respectively much more data about multipath nature of observed radio channel arise, since now the delay and Doppler shift data are known. Thus, from the TOA difference between corresponding rays and between groups of rays emanating from the scattering object we can make an assumption about its approximate width and relative position. For example, the TOA difference between group of diffracted and group of double diffracted rays in the case of illu-

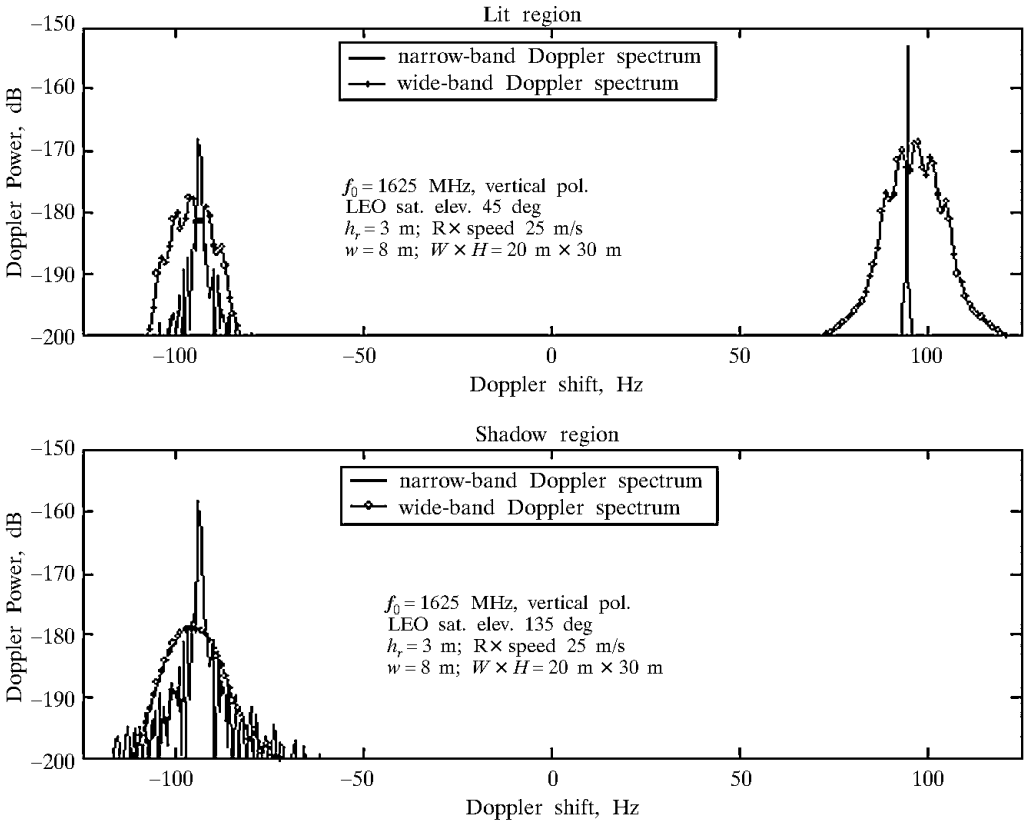

Fig. 5 Wide-band and narrow-band Doppler spectra of LEO satellite channel (fixed satellite) for vertical polarization in illuminated and shadow area, receiver speed 25 m/s away from the building, $(W \times H) = (20 \times 30)$ m^2, $h_r = 3$ m, $w = 8$ m

minated area is approximately 0,11 μs. Thus, the object width must be less than 33 m. Furthermore, the value of TOA difference between incident ray and the first arrived ray reflected from the object is about 0,04 μs, which corresponds to the distance difference of 12 m. Since this distance difference can reach the maximum value equals double receiver–object distance, one can immediately estimate that receiver is more than 6 m from the object. By introducing the effect of the incoming angle of incident ray derived from Doppler spectrum, estimation of the receiver position fix is about 8,5 m with direction from the object about 19,5 m wide, which closely matches the actual situation. Thus, if one possesses for example measured data, the geometrical influence concerning particular radio environment will be possible to assess. Inversely, if the geometrical and electrical characteristics of particular radio environment are known, the corresponding radio channel may obviously be modelled with high accuracy.

However, the LEO satellite in this example travels with velocity that is much higher than common vehicle or pedestrian speeds, which results in Doppler spectrum represented by upper diagram on Figure 6. In order to increase the resolution of data due to low velocity of the vehicle compared to the satellite velocity, the time window in the simulation had to be increased. Therefore, the number of points in FT was increased to 8196. Note that spectra obtained on Figure 5 are in reality shifted by the Doppler shift induced by the satellite movement that is of the order of tens of kilohertz for this example. In another words, the influence of the multipath on Doppler spectra becomes observable when receiver starts to move with a speed that induces an additional shift greater than Doppler resolution of the receiver. If we assume further that the receiver extracts the Doppler frequency by detecting the settlement of the strongest peak in a spectrum, the relative error Δ in the satellite Doppler shift in promilles that occurs due to the receiver mobility could be calculated as:

$$\Delta(‰) = \left| \frac{\nu_d - \nu_s}{\nu_s} \right| \cdot 1000, \qquad (2)$$

where ν_d denotes the shift detected while the receiver is moving and ν_s the true satellite frequency

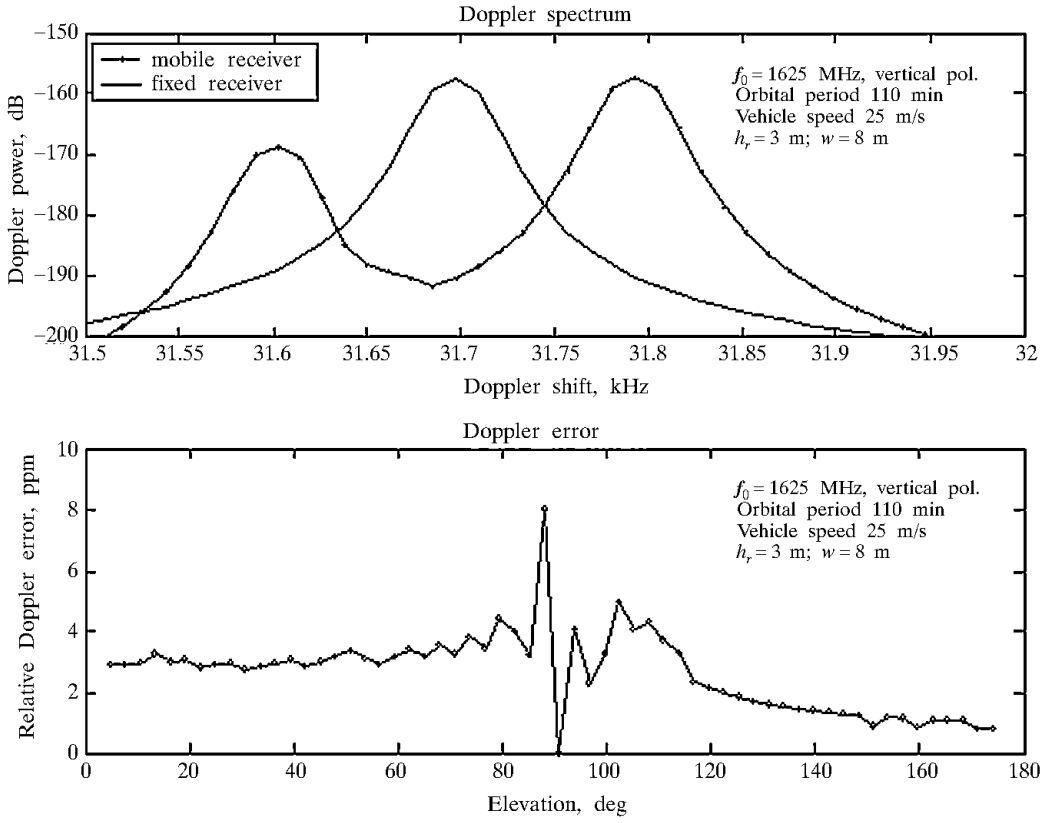

Fig. 6 Narrow-band Doppler spectra for situation according to the upper diagram of Figure 5, except the satellite is moving (upper diagram) and the estimated error in the satellite Doppler shift due to the receiver mobility with velocity 25 m/s (90 km/h)

shift. The lower diagram from Figure 6 shows the error Δ versus satellite elevation angle. The error Δ for this case is less than 10 ‰ and exhibits a poor dependence on elevation angle. Nonetheless, it is a few permilles lower in the shadow than in the illuminated area.

4 CONCLUSIONS

For simulations purposes of this paper, the narrow-band LEO satellite channel model from [1] is enhanced by a more precise equivalent Earth geometry, updated to the wide-band and then analysed according to the WPMS and FT procedure. The analysis shown clearly mirrors efficiency of the »ray-tracing« simulation of satellite radio channels, which thus enables us to predict values of important propagation channel parameters like coherence bandwidth and coherence time, or determining other channel statistics. Displayed time domain path losses, Doppler spectra and patterns of the relative power in frequency domain vividly point out the differences between two different situations of a LEO satellite's position.

Clearly, the major characteristics about particular radio environment can be concluded knowing only time domain path losses and Doppler power spectra or the channel scattering function. Inversely, if the geometrical and electrical characteristics of particular radio environment are well described by means of numerical values, the corresponding radio channel may obviously be modelled with high accuracy. Since the used methods are easily programmable they can serve as a basis for software modelling of various radio channel parameters and statistics, with parameters of radio environment or measured complex values of channel transfer function as the input data. Thus, the appliance of powerful procedures such as FT, »ray-tracing« and UGTD proved to be an elegant manner of achieving optimal QoS for given radio system.

5 APPENDICES

Appendix A.

In the equivalent Earth model, her real radius r_Z is exchanged with an effective radius r_{Zef} according to the relation:

$$r_{\mathrm{Zref}} = k r_{\mathrm{Z}} \tag{A.1}$$

where k represents a factor that cancels the curvature of the radio ray while propagating trough the troposphere layer. The relation for the k-factor is given by [10]:

$$k = \frac{1}{1 + r_Z \frac{1}{n}\frac{\mathrm{d}n}{\mathrm{d}h}\cos\alpha}, \tag{A.2}$$

where n denotes refractive index of the troposphere, α the transmitter elevation angle relative to the receiver and h the height above Earth surface. The radius of ray curvature in troposphere is a measure of the mean gradient of refractivity, and for standard atmosphere is equal to four radii of Earth. The refractivity index decrease with height and thus its gradient is negative. Its value is very close to unity (on sea surface and standard atmosphere is 1,0003) and can be neglected in relation above. So, assuming this conditions were met, the relation for the k-factor deduce to:

$$k = \frac{4}{4 - \cos\alpha}. \tag{A.3}$$

Appendix B.

The absolute path loss L between transmitter and receiver is a ratio of transmitted P_t and received power P_r and thus represents an inverse square absolute of the transfer function H of a radio channel. The path loss is commonly expressed in decibels,

$$L\left[\mathrm{dB}\right] = -20\log\left|\mathbf{H}(f)\right| = -10\log\frac{P_r}{P_t}. \tag{B.1}$$

Consequently, the time domain path loss L_t is defined via the inverse FT of the transfer function H as [2, 3]:

$$L_t\left[\mathrm{dB}\right] = 20\log\frac{\left|h(\tau)\right|}{0{,}902823 f_c}, \quad h(\tau) = \Im^{-1}\left\{\mathbf{H}(f)\right\}, \tag{B.2}$$

where sign $\Im^{-1}$ denotes inverse FT, f_c the clock frequency in megahertz, τ the time delay and h the channel impulse response. Relative power P_f in frequency domain is obtained as a square absolute FT of the impulse response envelope:

$$P_f(f) = \left|\Im\left\{\left|h(\tau)\right|\right\}\right|^2, \tag{B.3}$$

where sign $\Im$ denotes the FT operation.

Wide-band Doppler power spectrum P_{WD} can be calculated as:

$$P_{\mathrm{WD}}(\nu) = \int_{-\infty}^{+\infty}\left|\mathbf{S}(\tau,\nu)\right|^2 \mathrm{d}\tau \tag{B.4}$$

where ν is the Doppler frequency shift, while $\mathrm{S}(\tau,\nu)$ represents the propagation channel scattering function [7, 11] derived from the time-varying impulse response as:

$$\mathbf{S}(\tau,\nu) = \Im\left[h(\tau,t)\right]. \tag{B.5}$$

Narrow-Band Doppler power spectrum P_{ND} is readily obtained as a result of the FT of the time-varying channel transfer function H at central frequency f_0:

$$P_{\mathrm{ND}}(\nu) = \left|\Im\left[H(f_0,t)\right]\right|^2. \tag{B.6}$$

REFERENCES

[1] P. A. Tirkas, C. M. Wangsvick, C. A. Balanis, **Propagation Model for Building Blockage in Satellite Mobile Communication System**. IEEE Tr. on Antennas and Propagation, Vol. 46, No. 7, July 1998.

[2] W. Zhang, **A Wide-Band Propagation Model Based on UTD for Cellular Mobile Radio Communications**. IEEE Tran. on Antennas and Propagation, Vol. 45, No. 11, November 1997.

[3] R. J. Luebbers, W. A. Foose, G. Reyner, **Comparison of GTD Propagation Model Wide-Band Path Loss Simulation with Measurements**. IEEE Transactions on Antennas and Propagation, Vol. 37, No. 4, April 1989.

[4] D. C. Cox, R. P. Leck, **Correlation Bandwidth and Delay Spread Multipath Propagation Statistic for 910-MHz Urban Mobile Radio Channels**. IEEE Transactions on Communications, Vol. 23, No. 11, November 1975.

[5] D. C. Cox, **Delay Doppler Characteristic of Multipath Propagation at 910 MHz in a Suburban Mobile Radio Environment**. IEEE Transactions on Antennas and Propagation, Vol. AP-20, September 1972.

[6] E. Haas, **Aeronautical Channel Modeling**. IEEE Tr. on Vehicular Tech., Vol. 51, No. 2, March 2002.

[7] W. R. Braun, U. Dersch, **A Physical Mobile Radio Channel Model**. IEEE Transactions on Vehicular Technology, Vol. 40, No. 2, May 1991.

[8] B. Ulriksson, **Conversion of Frequency-Domain Data to the Time Domain**. Proceedings of the IEEE, Vol. 74, No. 1, January 1986.

[9] R. G. Kouyoumjian, P. H. Pathak, **A Uniform Geometrical Theory of Diffraction for an Edge in a Perfectly Conducting Surface**. Proceedings of the IEEE, Vol. 62, No. 11, November 1974.

[10] L. Boithias, **Radio Wave Propagation**. North Oxford Academic, 1987.

[11] R. Steele, **Mobile Radio Communications**. IEEE Press, USA, 1995.

[12] J. Doble, **Introduction to Radio Propagation for Fixed and Mobile Communications**. Artech House Boston–London, 1996.

Analiza satelitskog propagacijskog kanala s pomoću »ray-tracing« simulacije. U članku je opisana analiza satelitskog propagacijskog kanala s pomoću metoda potvrđenih u znanstvenoj literaturi kao što su: »ray-tracing«, jedinstvena geometrijska teorija ogiba i Fourierova transformacija. Ti su postupci lako programabilni te stoga mogu poslužiti kao osnova analitičke programske podrške za razne radio kanale. Da bi oslikali njihove mogućnosti, odabran je primjer radio kanala Low-Earth Orbit satelita za različite kutove elevacije (ozračeno ili područje sjene) koji emitira na prijenosnoj frekvenciji 1 625 MHz. U skladu s tim, prikazani su i analizirani dijagrami impulsnog odziva i Dopplerovi spektri. Može se zaključiti da se opisana simulacija može uspješno primijeniti pri analizi višestaznih radio kanala, posebno u slučajevima kada je potrebno odrediti temeljne parametre radio kanala poput koherentne širine pojasa ili koherentnog vremena.

Ključne riječi: satelitski propagacijski kanal, »ray-tracing«, jedinstvena geometrijska teorija ogiba, impulsni odziv, Dopplerov spektar

AUTHORS' ADDRESSES:

Mr. Sc. Zoran Blažević
Dr. Sc. Igor Zanchi, Red. Prof
Mr. Sc. Ivan Marinović
University of Split, Faculty of Electrical Engineering, Mechanical Engineering and Naval Architecture
Split, Ruđera Boškovića bb, 21000 Split, Croatia

Received: 2003–11–14